



Evaluation of Genetic Diversity in Olive Germplasm (*Olea europaea* L.) Using Image Processing and Molecular Markers Based on Physical Properties of Fruits and Stones

Ali Tanhaei¹, Ahmad Reza Dadras^{2*}, Hossein Sabouri¹, Ebrahim Gholamalipour Alamdari¹, Seyed Javad Sajadi¹, Hossein Hosseini Moghaddam¹

¹ Department of Plant Production, College of Agriculture Science and Natural Resources, Gonbad Kavous University, Gonbad, Golestan, Iran

² Crop and Horticultural Science Research Department, Olive Research Station of Tarom, Zanjan, Agricultural and Natural Resources Research and Education Center, AREEO, Zanjan, Iran

ARTICLE INFO

Article history:

Received: 5 January 2022,
Received in revised form: 24 April 2022,
Accepted: 15 May 2022

Article type:

Research paper

Keywords:

Image processing,
Fruit and stone physics,
Olive,
Molecular markers

ABSTRACT

Olive (*Olea europaea* L.) is a historic and significant Mediterranean tree that has been widely used for its curative properties and oily nature. Images of 150 randomly selected fruits were captured and processed in three replications to investigate the genetic diversity among 98 olive genotypes. The difference in all traits between genotypes was significant ($P < 0.01$), indicating a high level of genetic diversity among the olive genotypes. D1 outperformed other genotypes in terms of fruit area, major axis length, convex area, filled area, and equiv. diameter. The major axis length of the fruit exhibited a significant positive correlation with the perimeter, equivalent diameter, major axis length, and area of the stone ($P \leq 0.01$). Also, there was a significant, positive correlation between the minor axis lengths of the fruit and stone. The explained percentage of the traits' associated markers indicated that the fruits' major axis length had the highest cumulative coefficient (39%) with five bands. The IJS9-A and ScoT21-B genes regulated the most significant number of traits. The former regulated seven characteristics, i.e. fruit area, major axis length, minor axis length, convex area, filled area, equivalent diameter, and perimeter. In comparison, the latter regulated six characteristics, i.e. fruit area, major axis length, convex area, filled area, and the equivalent diameter of the fruit. Cluster analysis was used for categorizing genotypes into two groups. The findings of this study can be applied in hybridization and production programs for developing genotypes with more suitable fruits.

Introduction

The olive (*Olea europaea* L.) is an archaic member of the Oleaceae family. It is a Mediterranean oil plant widely used for its nutritional properties. Olive oil contains high amounts of oleic acid (Seifi, 2008). It is a permanent diploid species with a high degree of allogamy, resulting in a high level of heterozygosity. Olives can play a significant role in the human diet, reducing the risk of

cardiovascular disease, breast cancer, and colorectal cancer (Kaya et al., 2016). Iran is one of the origins of olives in the world, and it is critical to conserve the gene pool of this species. Moreover, it is important to identify and organize olive genotypes (Ghasemi, 2007). Iran is expected to establish a unique position in the olive cultivation industry because olive trees have shown a high level of compatibility with arid and

* Corresponding Author, Email: a.dadras@yahoo.com

semi-arid conditions in Iran (Arji et al., 2013). With 100,000 hectares under olive cultivation, Iran has gradually developed into one of the world's largest olive producers. The country has one of the world's most extensive olive genetic resources. Thus, it is critical to conduct genetic research on the various valuable genotypes in the country (Motaghi et al., 2012). Crossbreeding between genotypes is a common method for executing modification programs and achieving higher-quality genotypes in the olive industry. Given the distinctions between phenotype and genetics, parental selection is usually crucial in breeding olives (Milotic et al., 2005). Genetic diversity in plants is usually the result of genetic and environmental interactions. While genetic erosion occurs gradually in other plants with genetic diversity, it does not occur in the case of olives. This has resulted in a highly adaptable plant that can thrive in any environment and is frequently used in cultivation, modification and development programs (Angiolillo et al., 1999). Whereas olives exhibit a high degree of variation and diversity throughout Iran, determining their genotypes is challenging due to issues such as their lengthy juvenility stage and genomic complexity with 46 chromosomes ($n = 23$). As a result, molecular markers are highly targeted tools for evaluating and identifying genotypes (Jamshidi Jam et al., 2014; Omrani-Sabbaghi et al., 2007). Genetic diversity is critical for managing genetic resources for plant modification. Olives have a very high level of genetic diversity due to outcrossing and a high level of heterozygosity (Albertini et al., 2011). On the other hand, molecular markers are practical tools for genotype identification. The molecular composition of different olives necessitates the development of molecular properties for each genotype that agrees with the analysis of multiple locations in the genome and allows for precise species identification (Omrani-Sabbaghi et al., 2007). The association analysis directly assesses the relationship between genotypes and phenotypes in a plant by utilizing the existing continuity imbalance in natural populations and germplasm series to identify chromosomal regions involved in trait control. To ascertain the relationships between markers and traits, association analysis or mapping is used as an integrated method (Abbasi Holasou et al., 2018). Image processing is a valuable tool for determining the phenotypes of various plant and animal species today. Erkul et al. (2010) found that the traits of major axis length, minor axis length, area, equivalent diameter, perimeter, and grain weight had the most significant positive

impact on wheat yield.

Miri et al. (2020) measured major axis length, minor axis length, area, equivalent diameter, and perimeter traits to determine the genetic structure of the traits controlling wheat physics. They reported significant differences in the studied traits across generations. Sabouri and Sajadi (2022) and Sabouri et al. (2020) used image processing for determination of leaf area in aromatic plant and cereal, respectively.

Golmohammadi et al. (2018) evaluated the genetic diversity of a set of Iranian and foreign olive genotypes using ISSR markers. They propagated a total of 16 primers and 190 pieces, of which 172 were polymorphic. The analysis of molecular variance in AMOVA revealed that 7% of total changes were due to inter-group diversity, while 93% were due to inter-species diversity among olive cultivars and genotypes. The genetic relationships between the genotypes were analyzed using cluster analysis, classifying them into three major groups. ISSR markers, in general, can provide information about the genetic diversity and relationships between olive genotypes.

The broad-sense heritability and genetic variance of several primary flower and fruit traits were investigated in a two-year study using 20 olive genotypes at the Olive Research Station of Tarom in Zanjan Province, Iran. A total of 16 quantitative characteristics of the flower, fruit, stone, and leaves were investigated. The analysis of variance revealed significant differences in the traits of genotypes. The broad-sense heritability of fruits was nearly twice that of the flower. A positive genetic and phenotype correlation existed between the oil percentage and the flesh to stone ratio. Additionally, considerable diversity was observed among genotypes in terms of fruit and flower traits, allowing for the selection of superior cultivars based on genetic correlation and broad-sense heritability (Ahmadi et al., 2018).

Ebrahimnia et al. (2019) evaluated the morphological diversity of some olive genotypes in the Gorgan region of Iran by measuring 11 quantitative and 11 qualitative traits across 32 genotypes. Cluster analysis, classification, factor analysis, and principal component analysis were used for analyzing a total of 33 morphological traits associated with the leaf, stone, and fruit. The findings indicated a statistically significant difference ($P \leq 0.01$) between the measured traits. Additionally, the strongest correlation was found between the stone weight and diameter. Cluster analysis revealed that the 32 genotypes studied could be classified into six major clusters separated by a distance of 0.68.

Ebadi et al. (2019) investigated the genetic diversity of 30 genotypes (27 introduced and three landraces) and the quantitative and qualitative characteristics of 33 quantitative and qualitative traits. The analysis of variance revealed a significant difference in all traits, despite the high genetic diversity among genotypes. Correlation analyses revealed significant positive and negative correlations among some traits. Stepwise regression analysis revealed that the oil percentage in fresh matter depended on phenological variables such as color change and fruit ripening, whereas the performance trait depended on flower traits and percentage.

According to principal component analysis, ten components explained 90% of the total variation. Cluster analysis classified the genotypes into five groups separated by a factor of ten. The said research indicated that due to the high genetic diversity, crossbreeding could effectively use transgressive segregation to increase the oil content of fresh matter and, thus, create a new genotype.

The fruit, stone, and leaf morphological properties of four cultivars of *Lastroca* olive were evaluated. The results indicated that the genotypes differed genetically regarding the traits measured (Bencic et al., 2010).

Mottaghi et al. (2012) examined the genetic diversity of 49 olive samples belonging to ten genotypes using 20 RAPD primers. They discovered a high level of genetic diversity among genotypes. Nezamivand Chegeni et al. (2016) investigated the genetic diversity of 14 olive genotypes using morphological traits and discovered a significant positive correlation between the traits. The Ward method was used for classifying the genotypes into four groups. Since the *Konservolia* genotype outperformed other genotypes in terms of the studied traits, it was assigned to a separate group.

The AFLP marker was used for evaluating 18 genotypes in Molise, Italy, to determine the relationship between the cultivated genotype and the genotypes of adjacent regions. The genotypes were found to be similar using cluster analysis and principal component analysis. The findings revealed that the cultivated genotypes were highly similar, indicating that they were created by crossing very old genotypes in the past (Angiolillo et al., 2006).

Padula et al. (2008) quantified several essential traits, such as fruit and stone length, stone width and oil content, to identify superior genotypes among 134 genotypes in three regions of South-Central Italy. Eventually, the researchers identified 21 promising genotypes as superior.

Blazakis et al. (2017) used image processing to evaluate Greek genotypes for morphological evaluation and trait measurement of olives. The research allowed quantification of traits such as fruit and stone area, fruit and stone length, perimeter, equivalent diameter, nipple, fruit and stone shape, symmetry, and leaf properties. The results indicated that image processing was a viable method for determining olive traits.

Olive is a significant tree throughout the world, and particularly in Iran. Due to its medicinal, curative properties, and the benefits of olive oil, assessing genetic diversity and identifying superior olive genotypes is crucial for developing higher levels of efficiency in the crop. While numerous studies have been conducted on the genetic diversity of olives in Iran, each of them examined a small number of genotypes. The genetic diversity of its diverse germplasm was evaluated in this study using image processing and molecular markers based on the physical characteristics of the olive fruit and stone.

Materials and Methods

This study was conducted on 98 olive genotypes at Gonbad Kavous University in 2020-2021 (Table 1). The genotypes were obtained from the Olive Research Station of Tarom in Zanjan Province, Iran. A total of 150 olive fruits from each cultivar were randomly placed on white A4 paper in three replications to reduce background noise before image processing. The images were taken in a controlled environment using a fluorescent lamp to avoid casting the slightest shadow on the paper. This was accomplished using the primary camera on the Nokia 3.2 cellphone, which is of excellent quality and has a resolution of 13 MP. A concerted effort was made to capture images of all fruits simultaneously. Each image was taken from a constant height of 20 cm.

Transmission of images from the RGB space to grey space

Typically, images were saved in the RGB color space, which consisted of three vectors: red (R), green (G), and blue (B). The MATLAB software converted the color images to greyscale using the relationship $GL = 0.299 G + 0.587 R + 0.114 B$. In this equation, GL is the grey vector in the relationship mentioned above. The code $I = \text{rgb2gray}(\text{RGB})$ converted the images from the RGB color space to greyscale. Each of the vectors R, G, B, and GL had a value between 0 and 255. The full black and full white points were assigned values of zero and 255, respectively.

Between these values, the numbers indicated the degree of the greyness of a point. By omitting the

hue and saturation information and retaining the luminance values in this function, color images in

the RGB space were converted to greyscale images.

Table 1. List of studied genotypes of olives

Genotype number	Genotype	Origin	Genotype number	Genotype	Origin
1	Mosabi	Syria	21	Hamed	Egypt
2	Caridolia	Greece	23	Koroneiki	Greece
3	Corfolia	Spain	24	Leccino	Spain
4	Baladi	Syria	25	Amygdalolia	Greece
5	Oblonga	Spain	26	Arbequina	Spain
6	Kalamon	Greece	27	Konservolia	Greece
7	Cailletier	Italy	28	Mission	United States
8	Manzanilla F	Spain	29	Valanolia	Greece
9	Mavi	Syria	30	Grossane	France
10	Dan	Syria	31	Lucques	France
11	Jlot	Syria	32	Toffahi	Egypt
12	Khodeiri	Syria	33	Kaissy	Syria
13	Verdial de Jaén	France	34	Sorani	Syria
14	Piculin	French	35	Doebli	Syria
15	Nabali	Israel	36	Abou-satl	Syria
16	Voliotiki	Greece	37	Picual	Spain
17	Zard	Iran	38	Picudo	Spain
18	Rowghani	Iran	39	Manzanilla de sevilla	Spain
19	Mari	Iran	40	Manzanilla Cacerena	Spain
20	Shengeh	Iran	42	Lechin de granada	Spain

Genotype	Genotype number	Origin	Genotype	Genotype number	Genotype	Origin
Cornicabra	67	Spain	Fishmi	91	Ds14	Iran
Zard golooleh	68	Iran	Sevillana	92	Ds17	Iran
Souri	69	Syria	D1	93	GW1	Iran
Frantoio	70	Italy	Amficus Rudbar	94	KH-10	Iran
Cipressino	71	Italy	Fishimi Rudbar	95	KH-13	Iran
Piramidal	72	Greece	Ozine 2	96	T-H2	Iran
Dakal	73	Iran	Ozine 3	97	T-H4	Iran
Coratina	74	Italy	Tuscastan	100	T1	Iran
Dezful	75	Iran	Gorgon3	101	T2	Iran
Manzanilla	80	Spain	KH-BA	103	T6	Iran
Clonavis	81	Italy	T-MO1	104	T7	Iran
Gordal	82	Spain	T-MO3	105	T9	Iran
Agromanaki	83	Greece	T-MO4	106	T10	Iran
Tiaiki	84	Greece	T-MO12	109	T14	Iran
Patrini	85	Greece	Tmn2	112	T17	Iran
Chalkidikis	86	Greece	QG3	114	T19	Iran
Direh	87	Iran	QG8	116	T21	Iran
Amin	88	Iran	Bn1	118	T23	Iran
Meshkat	89	Iran	Bm5			
Derak	90	Iran	Ds7			

The following steps were utilized in the Image Processing Toolbox and included MATLAB R2016b to determine fruit properties:

Thresholds for segmentation of images

Segmentation of the images was performed using the $BW = \text{imbinarize}(I)$ code. By specifying a threshold value between 0 and 255, the background was made entirely white and the fruits completely black. As a result, a black and white image was created.

The Otsu method was used to determine the threshold limit for the $BW = \text{imbinarize}(I)$ function, and all values greater than it was

replaced with one, while the remaining values were replaced with zero. The threshold limit is chosen using this method to minimize the threshold variance between black and white pixels.

All zero values were replaced with ones in the $IM2 = \text{imcomplement}(IM)$ function, and vice versa. As a result, the fruits were white, and the background was black in the final image. This function was used to determine the complements

of the images.

When black points were detected in the fruit or white points were detected in the background (reducing measurement accuracy), the $BW2 = \text{imfill}(BW, \text{'holes'})$ function was used to eliminate them.

$BW2 = \text{bwpropfilt}(BW, \text{attrib}, \text{range})$ extracted the fruits from the images.

When the greyscale images were converted to black and white, the fruits were placed in different series of pixels, one for each olive fruit. Each fruit

was given a unique number. The fruits were extracted from the images using the MATLAB code ($BW2 = \text{bwpropfilt}(BW, \text{attrib}, \text{range})$). A criterion was used to eliminate all superfluous objects and accurately identify the fruits. After evaluating the images, the area of the fruits was used to determine their identity. All objects with areas smaller or greater than the determined limit were removed from the images using this function (Fig. 1).

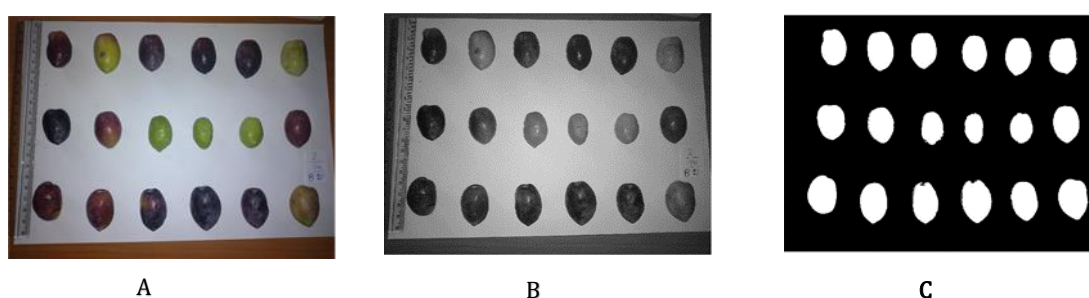


Fig. 1. Steps to perform image-processing analysis of olive fruits: A) Photos in space RGB; B) Gray image (binary); C) The final photo

Extraction of properties from each image segment identified

When the series of fruits contained within images were differentiated numerically, their characteristics were measured and calculated using the $\text{stats} = \text{regionprops}(BW, \text{properties})$ function (machine vision system).

Image calibration

By default, all 2D measurements of the fruits in the images were made in pixels, while rectangular and circular elements with specified dimensions (mm) were used to achieve the desired size. The images were calibrated, and all measurements were expressed in mm by substituting a specific element length equal to the real measured value for the pixel number.

Fruit and stone characteristics

Fruit and stone areas: The number of pixels contained within an intended area was reported as a scalar value. **Fruit and stone major axis length:** The length of the ellipse's major axis (in pixels) that has a second central moment equal to the intended area. **Fruit and stone eccentricity:** The eccentricity of an ellipse with a second central moment equal to the intended area, expressed as a scalar number. The eccentricity of an ellipse is equal to the ratio of the lengths of the

focal and major axes. Eccentricity is a value between 0 and 1. A zero-eccentricity ellipse is a circle, while a one-eccentricity ellipse is a direct line (Fig. 2).

Convex area: The smallest polygon that encompasses the fruit and stone area is called a convex area. The convex image's pixel count is specified as a scalar value. The convex image is the tiniest polygon that includes the intended area. **The area of the smallest rectangle encompassing the fruit- and stone-filled area:** The area contained within the smallest rectangle, including the intended image.

The equivalent diameter of fruit and stone: The equivalent diameter is the diameter of a circle whose area is equal to that of the intended region, as determined by the equation $\text{sqrt}(4 * \text{Area} / \pi)$.

The solidity of fruit and stone: Defined as the ratio of pixels within a convex area positioned within the intended area. Solidity is determined by the following relationship: $\text{Area} / \text{Convex Area}$.

The extent of fruit and stone: The ratio of the number of pixels in the image's intended area to the number of pixels in the smallest rectangle circumscribing this area as the fruit and stone limit.

The perimeter of fruit and stone: The perimeter of the fruit and stone is considered to be the entire length of the image's intended area.

The Image Processing Toolbox in the MATLAB

R2016b software was used to obtain the values of all traits.

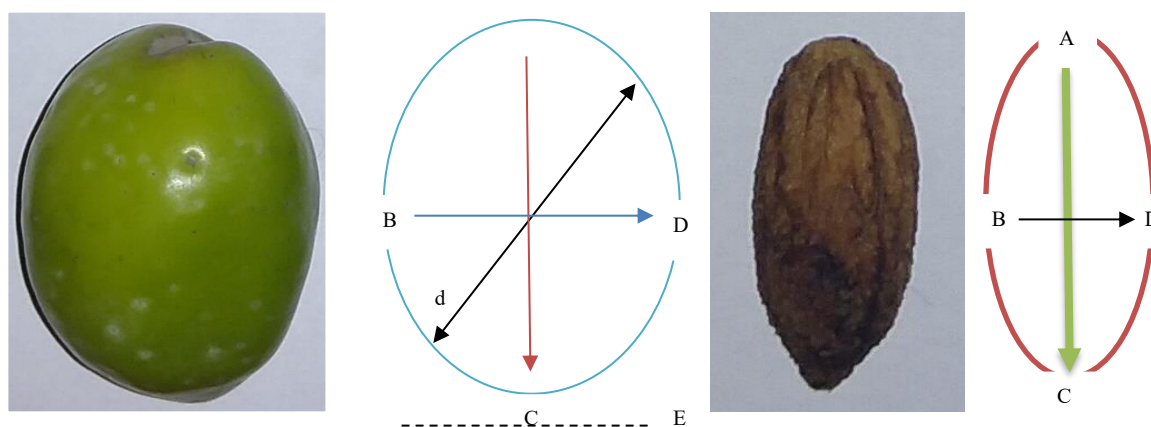


Fig. 2. Point distance (A-C), (B-D) Major Axis Length and Minor Axis Length, respectively. Line E represents eccentricity. Line d represents Equiv. Diameter.

DNA extraction, polymerase chain reaction and analyzing data

Fresh and young olive leaves were collected for DNA extraction. The leaves were then pulverized by liquid nitrogen and extracted using the CTAB method (Saghai-Marouf et al., 1984). Additionally, horizontal electrophoresis with 0.8% agarose was used to assess the extracted DNA's quality. The ScoT, CAAT, ITS, and ISJ markers were used in the PCR reaction. The amplified DNA was then placed on a 6% acrylamide gel. The gels were stained and kept in the refrigerator for scoring using the silver nitrate method (An et al., 2009). The morphological data and the relationship between the morphological and molecular traits were analyzed using the SPSS (Ver. 24) software (IBM Corp., 2010). Bonferroni correction (Bonferroni, 1936) was used for significant markers to prevent type I error. An extension of the method to confidence intervals was proposed by Dunn (1961). Statistical hypothesis testing was based on rejecting the null hypothesis if the likelihood of the observed data under the null hypotheses was low. If multiple hypotheses are tested, the chance of observing a rare event increases and, therefore, the likelihood of rejecting a null hypothesis incorrectly (i.e. making a Type I error) increases (Mittelhammer et al. 2000). For this purpose, the P value associated with related markers was tested against the significant critical value of Bonferroni. Accordingly, the two values (0.05 and 0.01) were divided by the number of evoked allele markers.

Results

The analysis of variance (ANOVA) on olive traits (Table 2) revealed a significant difference between fruit and stone traits ($P \leq 0.01$). The fruit area (4.347), the convex area of the fruit (4.319), the filled area of the fruit (4.347), and the fruit perimeter (4.370) exhibited the highest coefficient of variation (Table 2). All characteristics were statistically significant in the case of the stone ($P \leq 0.01$) (Table 2). The coefficient of variation was greatest for the stone area (3.803), convex area of stone (3.836), filled area of stone (3.803), and stone perimeter (2.365). The traits with the lowest coefficients of variation were eccentricity (0.671), solidity (0.225), and extent (0.750) (Table 2).

Ten percent of the genotypes with the highest trait values were further investigated. The D1 genotype demonstrated the highest values for fruit area (934.34 mm²), major axis length (41.738 mm), convex area (156096 pixel), filled area (154456 pixel), and the equivalent diameter of fruit (34.362 mm) (Table 3). The Mosabi genotype had the highest value of the minor axis length, indicating that its fruits were rounder than other genotypes. Furthermore, among the genotypes, Lucques, Hamed, Frantoio, and Caridolia had the highest values of eccentricity (0.815), solidity (0.991), fruit extent (0.795), and fruit perimeter (146.863 mm). Meanwhile, Koroneiki exhibited the lowest values of fruit area (204.33 mm²), minor axis length (13.331 mm), convex area (34352 pixel), filled area (33777 pixel), equivalent diameter (16.083), and fruit

perimeter (56.380 mm). Arbequina, Zard Golooleh, T-MO12, and Ozine 3 demonstrated the lowest values for major axis length (19.107 mm), eccentricity (0.413), solidity (0.975), and fruit extent (0.742), respectively.

Among the genotypes, the D1 genotype exhibited the highest values of stone area (236.649 mm²), major axis length (26.606 mm), convex area (40560.5 pixel), filled area (39119.6 pixel), equivalent diameter (17.294), and stone perimeter (692.78 mm) (Table 4). Toffahi, Lucques, Abou-Satl, and Derak genotypes had the highest values of fruit minor axis length (12.008 mm), stone eccentricity (0.930), stone solidity (0.982), and stone extent (0.761), respectively. Meanwhile, Koroneiki demonstrated the lowest

values of stone area (70.033 mm²), minor axis length (6.497 mm), convex area (11902.5 pixel), filled area (111576.9 pixel), and equivalent diameter (9.430). Arbequina exhibited the lowest values for major axis length (12.333 mm) and stone perimeter (33.636). Among genotypes, the T-H4, Tuscastan, and Lucques had the lowest eccentricity (0.594), solidity (0.954), and stone extent (0.653). Amygdalolia exhibited the highest fruit weight, flesh, length, and width in a study conducted by Zeinaloo et al. (2000) in the Kermanshah and Sarpol-zahab areas, while Mari, Arbequina, and Koroneiki had the lowest values for the traits mentioned above.

Table 2. Analysis of variance of 98 olive genotypes for fruit and stone traits

fruit						
S.O.V	df	Means of squares				
		Area	Convex Area	Eccentricity	Minor Axis Length	Major Axis Length
variation	97	63318.279**	1772334980.500**	0.0184**	35.836**	58.296**
Error	196	404.376	11179483.040	0.000	0.226	0.368
coefficient of Variation (%)		4.347	4.319	1.338	2.298	2.185
Means of squares						
S.O.V	df	Filled Area	Equiv. Diameter	Solidity	Extent	Perimeter
Genotype	97	1730242508.200**	42.075**	0.000**	0.000**	1028.709**
Error	196	11050033.751	0.273	0.000	0.000	15.343
coefficient of Variation (%)		4.347	2.190	0.226	0.449	4.370
Stone						
Stone S.O.V	df	Means of squares				
		Area	Major Axis Length	Minor Axis Length	Eccentricity	Convex Area
Genotype	97	3106.969**	22.642**	4.985**	0.011**	91185706**
Error	196	22.682	0.123	0.033	0.000	66589
coefficient of Variation (%)		3.803	2.037	1.983	0.671	3.836
Means of squares						
S.O.V	df	Filled Area	Equiv. Diameter	Solidity	Extent	Perimeter
Genotype	97	84901401**	7.319**	0.000**	0.001**	130.412**
Error	196	619816	0.053	0.000	0.000	1.163
coefficient of Variation (%)		3.803	1.853	0.225	0.750	2.365

**1% level of probability

Table 3. Mean comparison of olive fruit traits

10 % Superior												
	genotype	69	25	1	62	2	51	67	66	40	37	LSD
Area(mm ²)	value	934.36	876.34	835.92	748.32	745.49	739.47	719.30	670.70	644.39	643.05	32.381
Major Axis Length(mm)	genotype	69	25	51	1	2	62	67	37	11	63	
	value	41.738	40.548	38.103	37.384	37.291	36.530	34.038	33.358	32.681	32.320	0.977
Minor Axis Length(mm)	genotype	1	69	25	67	66	40	62	2	49	68	
	value	28.480	28.416	27.505	26.864	26.702	26.136	26.046	25.449	25.274	25.063	0.765
Eccentricity	genotype	31	112	3	4	19	72	75	6	51	73	
	value	0.815	0.789	0.785	0.781	0.770	0.770	0.769	0.756	0.756	0.750	0.014
Convex Area(pixel)	genotype	69	25	1	2	62	51	67	66	40	37	
	value	156096	146583	140253	126101	125368	123473	120150	112064	107567	107411	5384
Filled Area(pixel)	genotype	69	25	1	62	2	51	67	66	40	37	
	value	154456	144865	138183	123703	123234	122238	118904	110871	106522	106301	5352.7
Equiv. Diameter	genotype	69	25	1	62	2	51	67	66	40	37	
	value	34.362	33.309	32.540	30.799	30.702	30.483	30.202	29.151	28.579	28.482	0.842
Solidity	genotype	21	27	8	88	20	46	16	89	14	39	
	value	0.991	0.991	0.991	0.990	0.990	0.990	0.990	0.990	0.990	0.990	0.003
Extent	genotype	46	65	64	92	49	13	26	44	34	51	
	value	0.795	0.795	0.792	0.792	0.791	0.790	0.789	0.787	0.787	0.787	0.005
Perimeter(mm)	genotype	2	69	1	25	62	67	63	51	32	66	
	value	146.863	139.198	135.899	134.967	128.943	120.006	116.497	116.471	115.487	114.183	6.307
10 % lower												
Area(mm ²)	genotype	114	5	47	24	42	103	26	3	60	23	
	value	271.62	268.69	268.10	267.03	264.41	257.60	244.93	237.30	221.75	204.33	32.381
Major Axis Length(mm)	genotype	5	46	61	47	103	42	24	60	23	26	
	value	22.155	22.117	21.824	21.688	20.978	20.671	20.622	19.798	19.516	19.107	0.977
Minor Axis Length(mm)	genotype	112	64	74	47	103	5	114	60	3	23	
	value	16.039	15.958	15.930	15.705	15.576	15.374	15.104	14.091	13.645	13.331	0.765
Eccentricity	genotype	40	8	34	66	97	26	96	85	49	44	
	value	0.542	0.537	0.536	0.535	0.519	0.512	0.507	0.474	0.466	0.413	0.014
Convex Area(pixel)	genotype	114	47	5	24	42	103	26	3	60	23	
	value	45433	44960	44859	44565	44180	43188	41078	39623	37124	34352	5384
Filled Area(pixel)	genotype	114	5	47	24	42	103	26	3	60	23	
	value	44900	44416	44318	44141	43709	42584	40489	39228	36656	33777	5352.7
Equiv. Diameter	genotype	114	47	5	24	42	103	26	3	60	23	
	value	18.544	18.429	18.428	18.388	18.300	18.057	17.609	17.348	16.652	16.083	0.842
Solidity	genotype	74	94	91	29	73	87	6	61	2	84	
	value	0.983	0.983	0.983	0.982	0.982	0.982	0.982	0.981	0.976	0.975	0.003
Extent	genotype	112	74	2	100	75	105	61	84	23	73	
	value	0.763	0.762	0.761	0.761	0.760	0.758	0.751	0.745	0.743	0.742	0.005
Perimeter(mm)	genotype	61	64	74	42	26	5	3	24	60	23	
	value	68.177	67.845	65.722	65.056	64.770	62.741	62.407	62.074	58.912	56.380	6.307

The names and numbers of the genotypes are given in **Table 1**

Table 4. Mean comparison of olive stone traits

		10 % Superior										
	genotype	69	51	25	2	32	62	37	81	1	67	LSD
Area(mm ²)	value	236.649	223.217	213.348	206.943	194.975	178.065	172.084	171.558	169.055	159.390	7.668
Major Axis Length(mm)	genotype	69	51	25	2	62	4	72	37	32	6	
	value	26.606	26.319	25.540	24.416	22.005	21.902	21.633	21.368	20.628	20.378	0.566
Minor Axis Length(mm)	genotype	32	96	36	35	69	81	97	66	51	89	
	value	12.008	11.931	11.530	11.530	11.404	11.331	11.152	10.978	10.907	10.900	0.293
Eccentricity	genotype	31	4	14	43	75	72	73	3	6	51	
	value	0.930	0.922	0.916	0.913	0.908	0.908	0.906	0.906	0.906	0.905	0.009
Convex Area(pixel)	genotype	69	51	25	2	32	62	81	37	1	67	
	value	40560.5	38334.9	36887.0	35382.5	33021.6	30204.2	29402.9	29382.9	28715.9	26907.0	1314
Filled Area(pixel)	genotype	69	51	25	2	32	62	37	81	1	67	
	value	39119.6	36899.2	35267.7	34208.9	32230.5	29435.3	28446.6	28359.6	27945.9	26348.1	1267.7
Equiv. Diameter	genotype	69	51	25	2	32	62	37	81	1	67	
	value	17.294	16.723	16.419	16.172	15.685	15.017	14.717	14.709	14.625	14.211	0.372
Solidity	genotype	36	35	42	34	64	46	21	9	89	39	
	value	0.982	0.982	0.982	0.981	0.980	0.980	0.979	0.979	0.979	0.979	0.003
Extent	genotype	66	97	36	35	34	96	104	46	42	32	
	value	0.761	0.756	0.753	0.753	0.752	0.752	0.747	0.745	0.744	0.744	0.008
Perimeter(mm)	genotype	69	25	51	2	62	37	32	81	4	72	
	value	69.278	67.965	65.703	63.752	55.816	55.665	55.569	53.714	53.552	53.355	1.736
		10 % lower										
	genotype	3	74	42	24	116	103	26	61	60	23	
Area(mm ²)	value	83.393	81.786	80.829	79.876	79.768	79.175	76.017	73.964	72.155	70.033	7.668
Major Axis Length(mm)	genotype	97	23	85	44	103	60	61	42	24	26	
	value	13.986	13.846	13.830	13.397	13.394	13.129	13.120	13.077	12.885	12.333	0.566
Minor Axis Length(mm)	genotype	75	103	61	31	60	74	116	14	3	23	
	value	7.595	7.549	7.254	7.146	7.033	7.009	6.959	6.896	6.715	6.497	0.293
Eccentricity	genotype	26	27	17	33	36	35	85	44	96	97	
	value	0.769	0.768	0.767	0.766	0.736	0.736	0.637	0.631	0.603	0.594	0.009
Convex Area(pixel)	genotype	3	74	42	116	24	103	26	61	60	23	
	value	14221.0	14183.8	13604.0	13544.5	13514.2	13410.5	12846.2	12550.6	12215.3	11902.5	1314
Filled Area(pixel)	genotype	3	74	42	24	116	103	26	61	60	23	
	value	13785.4	13519.8	13361.6	13204.0	13186.2	13088.1	12566.0	12226.7	11927.6	11576.9	1267.7
Equiv. Diameter	genotype	3	74	42	24	116	103	26	61	60	23	
	value	10.283	10.173	10.113	10.058	10.054	10.019	9.814	9.684	9.568	9.430	0.372
Solidity	genotype	2	86	69	81	51	75	73	31	25	74	
	value	0.966	0.965	0.964	0.964	0.963	0.963	0.962	0.962	0.956	0.954	0.003
Extent	genotype	45	15	4	105	73	61	75	74	14	31	
	value	0.690	0.690	0.687	0.680	0.679	0.678	0.676	0.665	0.665	0.653	0.008
Perimeter(mm)	genotype	47	109	116	24	103	23	61	42	60	26	
	value	38.840	38.410	38.404	35.726	35.117	35.114	34.709	34.430	34.033	33.636	1.736

The names and numbers of the genotypes are given in **Table 1**

Correlation analysis of the fruit traits (Table 5 and Fig. 3) revealed a significant positive correlation between the major axis length of the fruit and the fruit area, convex area, and filled area of the fruit (0.960**). At a probability level of 1%, the equivalent diameter of the fruit had the highest correlation with the minor axis length, area, convex area, and filled area of the fruit (0.965** and 0.994**, respectively). Furthermore, at a probability level of 1%, the fruit perimeter had the highest correlation with the convex area (0.965**) and the fruit area (0.963**). At the 1% probability level, the eccentricity of the fruit had a significant negative correlation with its minor axis length (-0.390**) and extent (-0.494**).

The highest significant positive correlations were found between the stone area and its equivalent diameter (0.996**), the major axis length of the stone and its convex area (0.868**), the minor axis length of the stone, and its equivalent diameter (0.831**), and the perimeter of the stone and its equivalent diameter (0.962**). Meanwhile, the lowest correlations were found for the stone perimeter and extent (-0.104), stone solidity, and equivalent diameter (-0.190). At a 1% probability level, the eccentricity of the stone had a negative correlation with its minor axis

length (-0.507**), solidity (-0.420**), and extent (-0.651**). Additionally, there was a negative correlation between stone length and stone solidity (-0.449**) and stone extent (-0.220**) (Fig. 4).

The correlation between the fruit and stone traits revealed a significant positive correlation between the fruit's major axis length and the stone's perimeter, equivalent diameter, major axis length, and area, with coefficients of 0.895**, 0.879**, 0.858**, and 0.876**, respectively. At a 1% probability level (0.798**), the minor axis length of stone had the strongest positive correlation with the minor axis length of fruit. The stone solidity had the weakest correlation with fruit area (-0.196), convex area (-0.197), filled area (-0.196), and fruit equivalent diameter (-0.172).

Fruit eccentricity was significantly correlated with stone extent (-0.615**) and stone solidity (-0.436**). At a 1% probability level, the eccentricity of the stone had a significant negative correlation with the extent of the fruit (-0.377**), while the stone solidity had a significant negative correlation with the length of the fruit (-0.317**). The correlation results can be used to identify superior olive genotypes for use in olive modification programs.

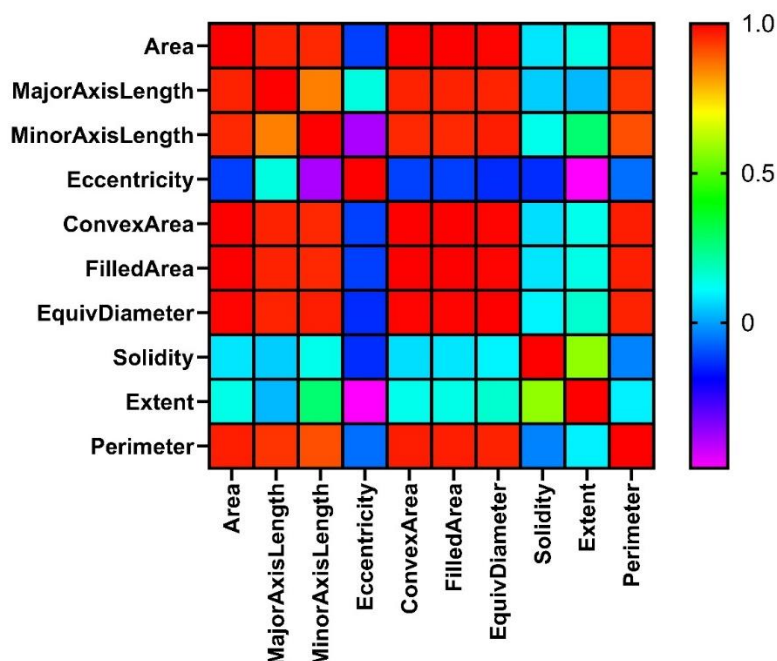


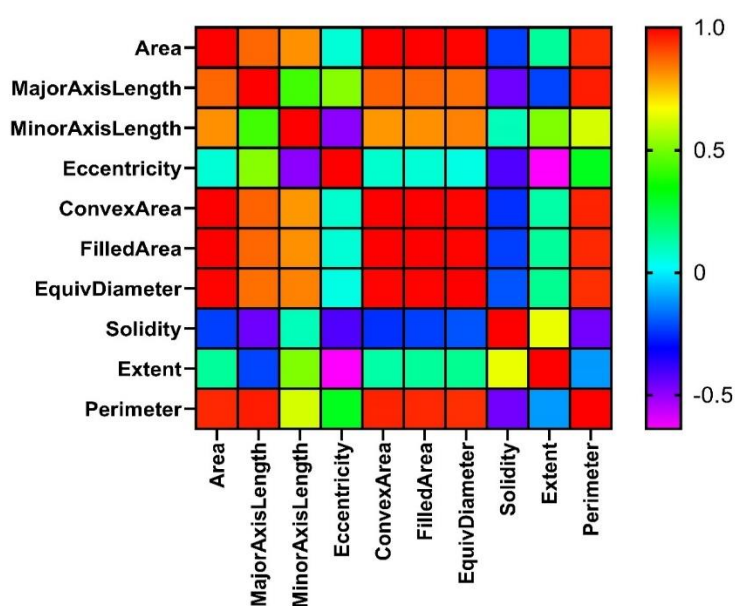
Fig. 3. Correlation between olive fruit traits

Table 5. Correlation between fruit and olive stone traits

Fruit Stone	Area	Major Axis Length	Minor Axis Length	Eccentricity	Convex Area	Filled Area	Equiv. Diameter	Solidity	Extent	Perimeter
Area	0.855**	0.876**	0.756**	0.095	0.856**	0.855**	0.846**	-0.047	0.050	0.823**
Major Axis Length	0.717**	0.858**	0.506**	0.521**	0.718**	0.717**	0.701**	-0.045	-0.153	0.712**
Minor Axis Length	0.723**	0.616**	0.798**	-0.423**	0.723**	0.723**	0.740**	-0.017	0.283**	0.671**
Eccentricity	0.009	0.220*	-0.236*	0.862**	0.009	0.009	-0.017	-0.014	-0.377**	0.063
Convex Area	0.855**	0.878**	0.752**	0.105	0.856**	0.855**	0.846**	-0.049	0.042	0.822**
Filled Area	0.855**	0.876**	0.756**	0.095	0.856**	0.855**	0.846**	-0.047	0.050	0.823**
Equiv Diameter	0.856**	0.879**	0.771**	0.077	0.857**	0.856**	0.856**	-0.035	0.070	0.825**
Solidity	-0.196	-0.317**	-0.032	-0.436**	-0.197	-0.196	-0.172	0.152	0.380**	-0.157
Extent	0.139	-0.034	0.301**	-0.615**	0.138	0.139	0.148	0.115	0.602**	0.143

The Ward method was used to classify the olive genotypes (Fig. 5). After categorizing the olive genotypes into two groups, the classification was confirmed using multivariate analysis of variance and the presence of a significant difference between the two groups. The Pillai's Trace, Hotelling's Trace, Wilks' Lambda, and Roy's Largest Root indices were significant between the

two groups. The first group contained 47 genotypes, including Iranian and foreign genotypes, indicating that the two types of genotypes for fruit and stone physics are similar. The second group contained a total of 51 genotypes. Figures 6 and 7 illustrate the fruit and stone characteristics and the average values for the genotypes included in each group.

**Fig. 4.** Correlation between olive stone traits

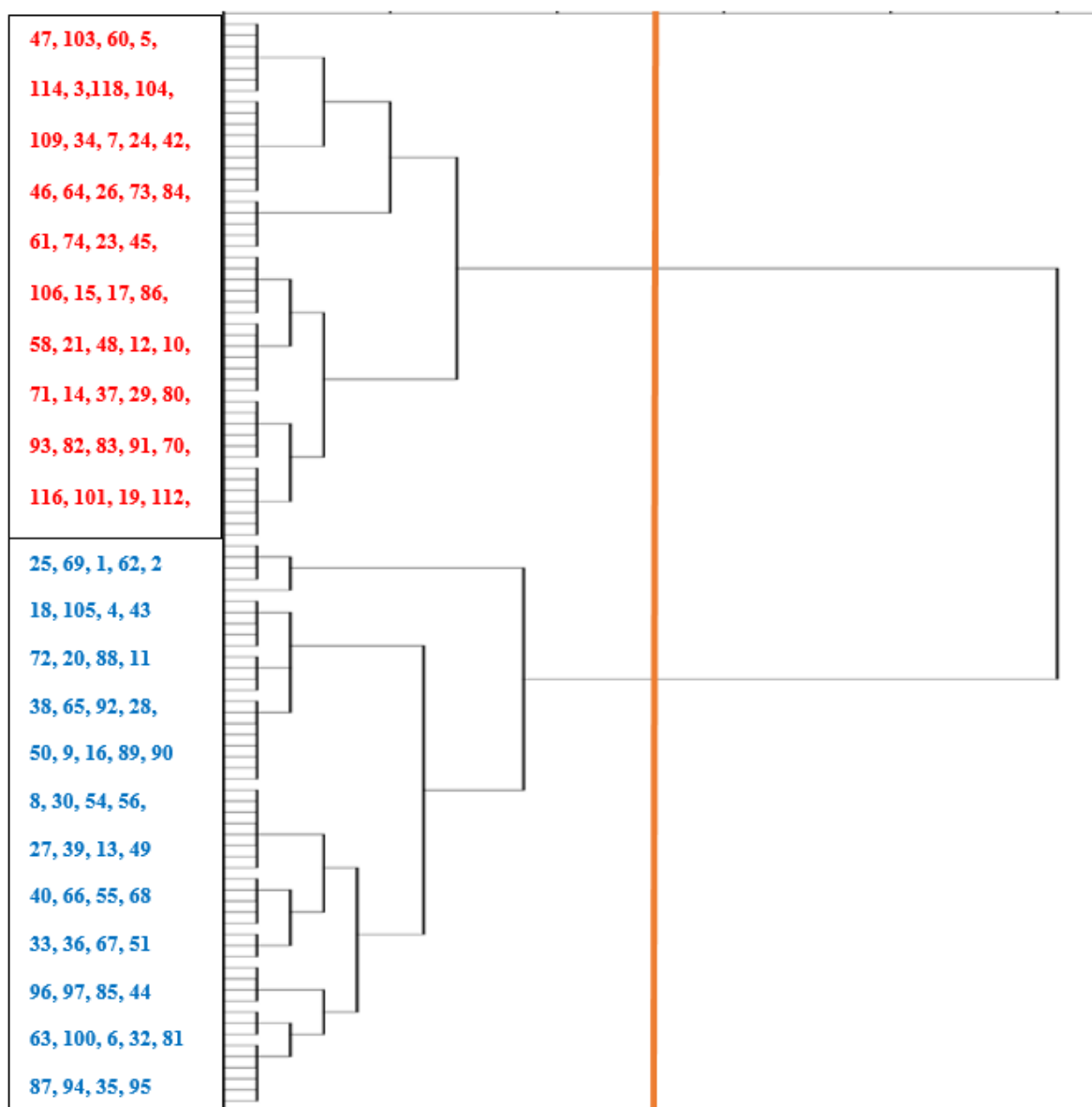


Fig. 5. Cluster analysis of 98 olive genotypes based on Ward’s method using fruit and stone traits

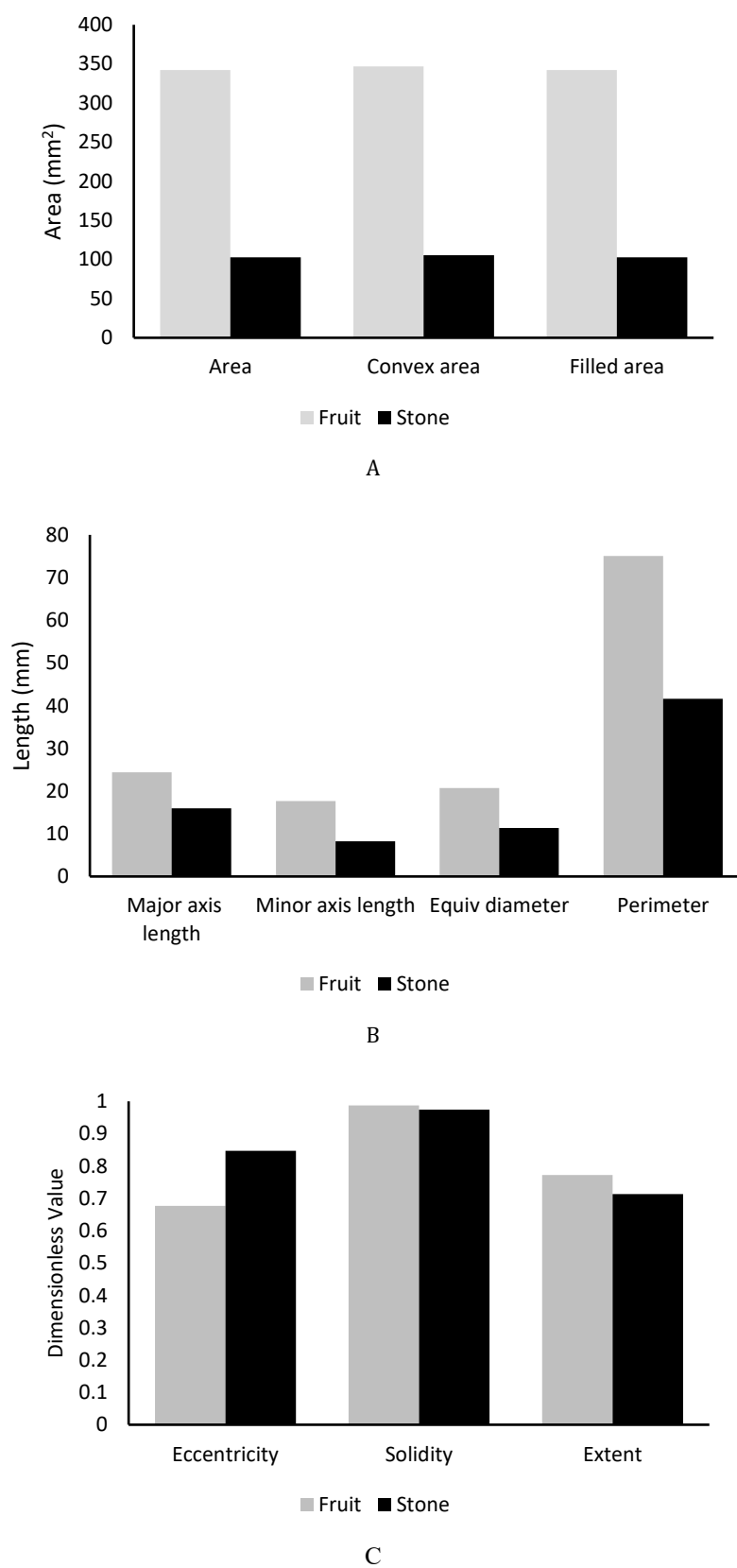


Fig. 6. Comparison of traits in first group of cluster analysis. A: Area, convex area, filled area; B: major axis length, minor axis length, Equiv. diameter, perimeter; C: Eccentricity, solidity, extent.

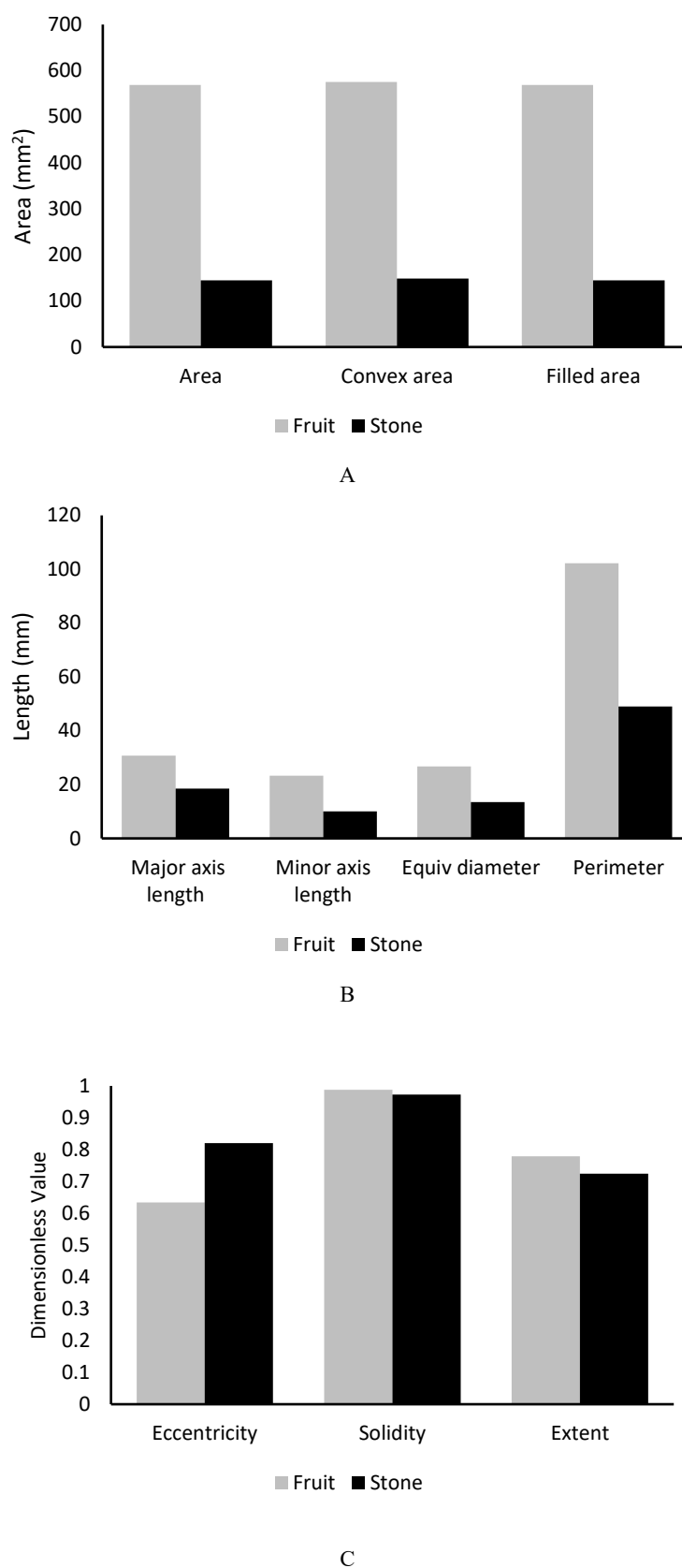


Fig. 7. Comparison of traits in second group of cluster analysis. A: Area, Convex area, filled area; B: Major axis length, Minor axis length, Equiv. diameter, Perimeter; C: Eccentricity, Solidity, Extent.

Association analysis

By including the fruit area as a dependent variable in the model, four bands of IJS9-A, SCoT7-B, SCoT21-B, and ITS4-C explained 31.5% in this trait. It was increased by three bands, while it was decreased by one band. SCoT14-E, CAAT16-A, and SCoT21-B (all with a decreasing effect) and the two bands ITS4-C and IJS9-A (both with an increasing effect) played a significant role in controlling the fruit's major axis length and could account for 39% of its variation. All three bands associated with fruit's minor axis length, namely IJS9-A, SCoT7-B, and CAAT10-A, increased it, accounting for 25% of the variation in this trait. The ITS5-E, SCoT4-C, CAAT6-E, and IJS13-A alleles may contribute to the fruit's eccentricity and account for 34.3%. Each of the four bands containing eccentricity information had a decreasing effect. The ITS4-C, SCoT7-B, SCoT21-B, and IJS9-A could each control 31.5% of the convex

area's changes (three bands increased it, while one lowered it). The bands IJS9-A, SCoT7-B, SCoT21-B, and ITS4-C, accounted for 31.5% of the changes in the filled area (three improved the trait, while the fourth decreased it). SCoT7-B, SCoT21-B, and IJS9-A contributed to controlling 32.2% of the fruit's equivalent diameter (three bands boosted it, while one band lowered it). The CAAT12-B and IJS5-D were significantly incorporated into the model, controlling 21.4% of it, with one band having a decreasing effect and the other having an increasing effect. The ITS2-C, IJS14-B, IJS10-F, and ITS2-F alleles explained 34.8% of the fruit extent (two of them increased it, while the remaining two reduced it). The model included the fruit perimeter trait as a dependent variable and the bands as an independent variable. IJS9-A, CAAT16-A, SCoT21-B, and ITS4-C bands accounted for 31.1% (two of them increased it, while the remaining two decreased it) (Table 6).

Table 6. Regression analysis of olive fruit and stone traits

Fruit			
Traits	Informative markers	F test	R Square
Area	SCoT21-B, SCoT7-B, IJS9-A, ITS4-C	10.716**	0.315
Major Axis Length	SCoT21-B, ITS4-C, CAAT16-A, IJS9-A, SCoT14-E	11.772**	0.390
Minor Axis Length	SCoT7-B, IJS9-A, CAAT10-A	10.462**	0.250
Eccentricity	CAAT6-E, SCoT4-C, ITS5-E, IJS13-A	12.113**	0.343
Convex Area	SCoT21-B, SCoT7-B, ITS4-C, IJS9-A	10.685**	0.315
Filled Area	SCoT21-B, SCoT7-B, IJS9-A, ITS4-C	10.716**	0.315
Equiv Diameter	SCoT21-B, SCoT7-B, ITS4-C, IJS9-A	11.048**	0.322
Solidity	CAAT12-B, IJS5-D	12.921**	0.214
Extent	IJS10-F, IJS14-B, ITS2-C, ITS2-F	12.417**	0.348
Perimeter	SCoT21-B, CAAT16-A, IJS9-A, ITS4-C	10.477**	0.311
Stone			
Area	SCoT21-B, CAAT16-A	11.424**	0.194
Major Axis Length	SCoT21-B, ITS4-C	11.142**	0.190
Minor Axis Length	SCoT7-B	12.422**	0.115
Eccentricity	CAAT6-E, SCoT4-A	11.882**	0.200
Convex Area	SCoT21-B, CAAT16-A	11.247**	0.191
Filled Area	SCoT21-B, CAAT16-A	11.424**	0.194
Equiv. Diameter	SCoT21-B, CAAT16-A	11.686**	0.197
Extent	ITS13-E	8.310**	0.080
Perimeter	SCoT21-B	12.355**	0.114
Area	SCoT21-B, CAAT16-A	11.424**	0.194

By treating the stone area as a dependent variable and the bands as variables, two bands, CAAT16-A and SCoT21-B, were able to control 19.4% of the variations, both with a decreasing effect. SCoT21-B (with a decreasing trend) and ITS4-C (with an

increasing trend) bands could account for 19% of the stone major axis length variation. Additionally, band SCoT7-B had an increasing effect on the minor axis length of stone by 11.5%. By reducing this trait, the bands CAAT6-E and

SCoT4-A could control 20% of changes in eccentricity. SCoT21-B and CAAT16-A bands could account for 19.1% in stones' convex area, with both bands exhibiting a negative decreasing trend.

Two bands could account for 19.4% of the variation in the filled area of stone. SCoT21-B and

CAAT16-A were the bands used. SCoT21-B and CAAT16-A could negatively control 19.7% of the variations in the equivalent diameter. ITS13-E negatively regulated 8% of changes in the stone extent. SCoT21-B was found to be capable of controlling 11.4% of changes in the stone perimeter in a decreasing trend (Table 7).

Table 7. List of significant molecular marker bands and fruit and stone traits

Fruit		
Band	No. traits	Dependent traits
ScoT21-B	6	Area, Major Axis Length, convex Area, Filled Area, Equiv. Diameter, Perimeter
IJS9-A	7	Area, Major Axis Length, Minor Axis Length, convex Area, Filled Area, Equiv. Diameter, Perimeter
SCoT7-B	5	Area, Minor Axis Length, convex Area, Filled Area, Equiv Diameter,
ITS4-C	6	Area, Major Axis Length, convex Area, Filled Area, Equiv Diameter, Perimeter
SCoT14-E	1	Major Axis Length
CAAT16-A	2	Major Axis Length, Perimeter
CAAT10-A	1	Minor Axis Length
CAAT6-E	1	Eccentricity
CAAT12-B	1	Solidity
IJS5-D	1	Solidity
IJS10-F	1	Extent
IJS14-B	1	Extent
ITS2-C	1	Extent
ITS2-F	1	Extent
Stone		
ScoT 21-B	6	Area, Major Axis Length, convex Area, Filled Area, Equiv Diameter, Perimeter
CAAT16-A	4	Area, convex Area, Filled Area, Equiv Diameter
ITS4-C	1	Major Axis Length
SCoT7-B	1	Minor Axis Length
CAAT6-E	1	Eccentricity
SCoT4-A	1	Eccentricity
ITS13-E	1	Extent

Discussion

Analysis of variance revealed a high level of genetic diversity among the olive genotypes. The coefficient of variation indicated that these traits changed significantly and were highly effective in fruit traits. On the other hand, the coefficients of variation for solidity (0.226), eccentricity (1.338), and extent (0.449) were the lowest.

All traits were significant at the 1% probability level in this study, indicating that they can aid in the identification of olive genotypes and their genetic diversity. Thus, they can be used for the discrimination and classification of genotypes. Ebadi et al. (2019) also reported a high level of genetic diversity in fruit length, fruit diameter, fruit weight, stone length, stone weight, and stone diameter in their study of olive genetic diversity and identification of the best genotypes. Ebrahimi et al. (2019) discovered a significant difference between the fruit and stone length, weight, length/diameter ratio, and flesh percent of 32 olive genotypes.

The variance analysis and averages comparison revealed significant fruit and stone traits differences between the studied germplasm. The D1 genotype produced the largest olives. The fruit size had a significant effect on performance. Mosabi genotypes had a longer minor axis. The results indicated that the major axis length of the fruit, the minor axis length of the fruit, equivalent diameter, and the fruit perimeter all had a significant effect on the fruit's performance and size. Ebadi et al. (2019) assessed the genetic diversity of 30 olive genotypes from Iran and non-Iranian origin. They discovered that *Amygdalolia* (3.33 cm) and *Arbequina* (1.67cm) had the largest and smallest fruit lengths, respectively. The Mosabi and Koroneiki genotypes had the largest fruit diameters, averaging 2.47 and 1.2 cm, respectively.

Torkzaban et al. (2010) used molecular markers to assess the genetic diversity of olive genotypes at the Olive Research Station of Tarom. The findings indicated a high degree of genetic variation between Iranian and foreign genotypes. As a result, they are suitable for genetic modification programs.

Classification of genotypes and cluster analysis can benefit plant breeding programs for a wide variety of traits, allowing for the determination of similarity and the utilization of inherent diversity (Rallo et al., 2018).

The first group of genotypes had lower fruit and stone traits values than the second group. In the first group, Gorgon3, Amficis Rudbar, and Fishmi Rudbar genotypes were superior genotypes for the classification's intended traits. Meanwhile, the

D1 genotype had the highest values of the second group of genotypes.

According to Table 7, IJS9-A7 increased its control over fruit area, major axis length, minor axis length, convex area, filled area, equivalent diameter, and perimeter. SCoT21-B exerted decreasing control over the six traits of the convex area, perimeter, convex area, filled area, and the equivalent diameter. If the fruit is exhibited an increasing trend, band SCoT7-B 5 controls the area, perimeter, convex area, filled area, and the equivalent diameter. ITS4-C exerted increasing control over the area, major axis length, convex area, filled area, equivalent diameter, and fruit perimeter. CAAT16-A controlled the length and perimeter of the fruit's major axis in a decreasing trend.

Additionally, SCoT14-E influenced the length of the fruit's major axis in a negative direction, whereas CAAT10-A influenced the length of the fruit's minor axis in a positive direction. CAAT6-E and CAAT12-B bands, respectively, controlled eccentricity in a negative and positive direction, while IJS5-D controlled solidity in a decreasing direction. IJS10-F and IJS14-B had a decreasing effect on fruit extent, whereas ITS2-C and ITS2-F had an increasing effect.

ScoT21-B had a decreasing effect on the area, major axis length, perimeter, convex area, filled area, and the equivalent diameter of the stone. ITS4-C and SCoT7-B exerted positive and increasing control over the stone's major and minor axes, respectively. CAAT6-E and SCoT4-A decreased the stone eccentricity, while ITS13-E decreased the stone length.

Conclusion

According to the analysis of variance results, all traits were significant at the 1% probability level, indicating a high degree of genetic diversity among the genotypes. The evaluation of 10% of genotypes with the highest trait values revealed that the D1 genotype performed the best. The association analysis revealed that IJS9-A and SCoT21-B were responsible for controlling the traits of fruits and stones, respectively. Cluster analysis was used to classify the genotypes into two groups. The information obtained from this study can be applied to olive cultivar hybridization programs.

Acknowledgments

The authors wish to express their gratitude to the Olive Research Station of Tarom for supplying the necessary plant materials for the research.

Conflict of Interest

The authors declare that they have no conflict of

interest.

References

- Arji I, Zeinanloo AA, Hajiamiri A, Najafi M. 2013. An investigation into different olive cultivars responses to Sarpole Zehab environmental condition. *International Journal of Plant Production* 35, 17-27.
- Abbasi Holasou H, Abdollahi Mandoulakani B, Hassanzadeh Ghorrtapeh A. 2018. Association analysis for yield and plant characteristics in Iranian flax genotypes (*Linum usitatissimum* L.) using IRAP and REMAP markers. *Journal of Molecular and Cellular Researches* 33(4), 585-597.
- Ahmadi Z, Soleimani A, Saba J, Taheri M. 2018. Correlation between Flower and Fruit Characteristics in some Olive Cultivars in Climatological Conditions of Tarom. *Seed Plant Journal* 33(3), 283-297.
- Angiolillo A, Reale S, Pilla F, Baldoni L. 2006. Molecular analysis of olive cultivars in the Molise region of Italy. *Genetic Resources and Crop Evolution* 53, 289-295.
- Angiolillo A, Mencuccini M, Baldoni L. 1999. Olive genetic diversity assessed using amplified fragment length polymorphism. *Theoretical and Applied Genetics* 98, 411-421.
- Albertini E, Torricelli R, Bitocchi E, Raggi L, Marconi G, Pollastri L, Di Minco G, Battistini A, Papa R, Veronesi F. 2011. Structure of genetic diversity in (*Olea europaea* L.) cultivars from central Italy. *Molecular Breeding* 27, 533-547.
- An ZW, Xie LL, Cheng H, Zhou Y, Zhang Q, He XG, Huang HS. 2009. A silver staining procedure for nucleic acids in polyacrylamide gels without fixation and pretreatment. *Analytical Biochemistry* 391(1), 77-79.
- Bencic D, Lolic T, Sindrak T. 2010. Morphological diversity of olive (*Olea europaea* L.) variety Lastovka phenotypes in the north-western part of the island of Korcula. *Seed Science* 26, 153-159.
- Betul Kaya H, Cetin O, Sozer Kaya H, Sahin M, Sefer F, Tanyolac B. 2016. Association mapping in Turkish olive cultivars revealed significant markers related to some important agronomic traits. *Biochemical genetics* 54, 506-533.
- Bonferroni, C. E. 1936. *Teoria statistica delle classi e calcolo delle probabilità*, Pubblicazioni del R Istituto Superiore di Scienze Economiche e Commerciali di Firenze.
- Blazakis KN, Kosma M, Kostelenos L, Bufacchi M, Kalaitzis P. 2017. Description of olive morphological parameters by using open access software. *Plant Methods* 13, 111.
- Ebrahimnia S, Seifi E, Hemmati Kh, Fereidooni H. 2019. Study of morphological diversity in some olive genotypes of Gorgan region. *Journal of Plant Production* 26(4), 97-113.
- Dunn, O. J. 1961. Multiple comparisons among means. *Journal of the American Statistical Association* 56 (293), 52-64.
- Ebadi R, Bihamta MR, Bahmani R. 2019. Assessment of genetic variation between some of the Iranian and foreign olive cultivars with using of quantitative and qualitative traits. *International Journal of Horticultural Science* 49(4), 845-858.
- Erkul A, Unay A, Konak C. 2010. Inheritance of yield and yield components in a bread wheat (*Triticum aestivum* L.) cross. *Turkish Journal of Field Crops* 15, 137-140.
- Golmohammadi M, Sofalian O, Ahmadi J, Taheri M, Ghanbari A, Rasoli V. 2018. Evaluation of genetic variation in some Iranian and foreign cultivars and promising genotypes of Olive using ISSR markers. *International Journal of Sciences* 13(4), 479-487.
- Ghasemi A. 2007. Identification and collection of native varieties and wild species of almond from Feridunshahr. *Proceedings of the 5th Iranian Horticultural Sciences Congress*. University of Shiraz. Iran. 610p.
- IBM Corp. Released. 2010. *IBM SPSS Statistics for Windows, Version 19.0*. Armonk, NY: IBM Corp.
- Jamshidi JF, Rabiei V, Jafari H, Fotovat R, Taheri M. 2014. Genetic Diversity Among Olive Clones of Zard and Rowghani Cultivars Using Microsatellite Markers. *Seed Plant Journal* 30(2), 327-345.
- Motaghi L, Mazinani SM, Jabari H. 2012. Evaluation of genetic diversity in some Iranian olive cultivars using RAPD markers. *Plant Ecology Systematics* 33, 91-104.
- Miri A, Sabouri H, Hosseini Moghaddam H, Soughi H, Mollahshahi M, Sajadi J. 2020. Genetic structure of wheat (*Triticum aestivum* L.) grain characteristics by using image processing and generation mean analysis techniques. *Journal of Genetic Resources* 6(2), 131-141.
- Milotic A, Setic E, Persuric D, Poljuha, D., Sladonja, B., and Brscic, K. 2005. Identification and characterization of autochthonous olive varieties in Istria. *Annales Series Historia Naturalis* 15 (2), 251-256.
- Mittelhammer, R, Judge C, George G, Douglas J. 2000. *Econometric Foundations*. Cambridge University Press. pp. 73-74.
- Nezamivand M, Moradi H, Sadeghi H. 2016. Genetic diversity of olive varieties based on morphological traits. *Horticultural Sciences Congress*. Shahid Chamran University of Ahvaz, Iranian Association of Horticultural Sciences.
- Omrani-Sabbaghi A, Shahriari M, Falahati-Anbaran M, Mohammadi SA, Nankali A, Mardi M, Ghareyazie B. 2007. Microsatellite markers based assessment of genetic diversity in Iranian olive (*Olea europaea* L.) collection. *Scientia Horticulturae* 112, 439-447.
- Padula G, Giordani E, Bellini E, Rosati A, Pandolfi S, Paoletti A, Pannelli G, Ripa V, De Rose F, Perri E, Buccoliero A, Mennone C. 2008. Field evaluation of new olive (*Olea europaea* L.) selections and effects of genotype and environment on productivity and fruit characteristics. *Horticultural Science* 22, 87-94.
- Rallo L, Barranco D, Díez C.M, Rallo P, Suárez M.P, Trapero C, Pliego-Alfaro F. 2018. Strategies for Olive (*Olea europaea* L.) Breeding: Cultivated Genetic

Resources and Crossbreeding. J. M. Al-Khayri et al. (eds.), *Advances in Plant Breeding Strategies: Fruits*, https://doi.org/10.1007/978-3-319-91944-7_14

Sabouri H, Sajadi S. J. 2022. Image processing and area estimation of chia (*Salvia hispanica* L.), quinoa (*Chenopodium quinoa* Willd.), and bitter melon (*Momordica charantia* L.) leaves based on statistical and intelligent methods. *Journal of Applied Research on Medicinal and Aromatic Plants* 30, 100382

Sabouri H, Sajadi, S. J, Jafarzadeh M. R, Rezaei M, Ghaffari S, Bakhtiari S. Image processing and prediction of leaf area in cereals: A comparison of artificial neural networks, an adaptive neuro-fuzzy inference system, and regression methods. *Crop Science* 61(2), 1013-1029

Saghai-Marouf MA, Soliman KM, Jorgensen RA, Allard RW .1984. Ribosomal DNA sepace length polymorphism in barley: Mendelian inheritance, chromosomal location and population dynamics.

Proceedings of the National Academy of Sciences 81(24), 8014–8019.

Seifi E .2008. Self-Incompatibility of olive. Discipline of wine and horticulture school of agriculture, food, and wine faculty of science, University of Adelaide, Australia.

Torkzaban B, Ataie S, Saboura O, Azimi M, Hoseini Mazinani M. 2010. Study of variation of some unknown olive genotypes in collection of Tarom Research Station in Iran, applying morphological markers. *Iranian Journal of Biology* 23(4), 520-531

Zeinaloo A, Arji A, Haji Amiri, A. 2000. Evaluation and examination of olive adaptability in whether condition of Sarepolezahab. The First Native Festival and Congress of Olive. Ghazvin. Iran

COPYRIGHTS ©2021 The author(s). This is an open access article distributed under the terms of the Creative Commons Attribution (CC BY 4.0), which permits unrestricted use, distribution, and reproduction in any medium, as long as the original authors and source are cited. No permission is required from the authors or the publishers

